

Discrimination of Multi-Reaction Pathways in the Oxidation of Carbon Monoxide on Zinc Oxide*

Masaki HAKOZAKI**, Boris GOLMAN***, Tohru KANNO****
and Masayoshi KOBAYASHI****

(Received April 28, 1992)

Abstract

Anomalous behavior of heterogeneously catalyzed CO oxidation on ZnO at the steady state and the transient state has been interpreted by the multi-reaction pathway model based on the different intermediates (*Is*). The reaction mechanism consists of a Langmuir-Hinshelwood (L-H) part, in which *Is* is O (neutrally adsorbed oxygen), and an Eley-Rideal (E-R) part with O⁻. The mode of transient response curve is sensitively shifted among a monotonous, an overshoot, a false start and a complex type according to the concentrations of CO and O₂. The proposed model consistently explains the anomalous steady state rate kinetics and the mode of transient response curves, and all the kinetic parameters of the reaction sequences are evaluated by using a computer simulation technique, indicating the good fit to the experimental curves.

1. INTRODUCTION

Recent progress of the techniques for characterizing solid surfaces has visualized surface structure in detail and revealed diverse degree of coordinative unsaturation. The heterogeneity of surface ions of metal oxides and supported metals may reasonably induce multi-reaction pathways caused by the variety of adsorbed species. The specific species (designate *Is*) adsorbed on the surface will selectively control the reaction pathway according to the surrounding conditions¹⁻³⁾. The complexity of the reaction routes progressed in heterogeneous surfaces has brought about a complexity of the mode of steady state rate kinetics and transient response curves obtained and thereby a difficulty of the discrimination of multi-reaction pathways. The regulation of reaction routes is, however, available to raise reaction yield and selectivity to important products.

Very recently, Kherbeche et al¹⁾ have demonstrated the hydrodenitrogenation (HDN) of pyridine to be in multi-reaction pathways depending on the temperature of treatment (T_R) of

* The paper was presented at the National Meeting of the Chemical Engineers of Japan in 1991.

** Chemical Environmental Engineering.

*** N. D. Zelinsky Institute of Organic Chemistry, Moscow, CIS.

**** Department of Industrial Chemistry.

Mo and Ni-Mo-based catalysts under H_2 . The reduction by H_2 has two roles: the removing sulfur at the edges of the supported MoS_2 phase and the creating the coordinative unsaturated Mo sites. The kinetics shows, that the rate determining step to be the piperidine transformation into n-pentylamine at low T_R , where as another route with out any piperidine intermediate is available at high T_R . These results suggest that the number of coordination unsaturations can regulate the reaction route according to the reaction conditions.

In the present study, our interest is focused on the discrimination of multi-reaction pathways, the elevating of the selectivity to a desired reaction route, and the investigation of specific species which can control both the reaction pathways and the selectivity to desired products. To discriminate the multi-reaction pathways, one of the most useful tools may be the transient response method⁴⁻¹⁰ and it has been applied to CO-oxidation on ZnO ¹¹⁻¹³.

2. EXPERIMENTAL

2-1. Procedure

The zinc oxide used in this study was commercially prepared by Kadox 25. The catalyst particle size was 20-42 mesh and its BET surface area was $20\text{ m}^2/\text{g}$, and it was confirmed to be an n-type semiconductor by measuring the electrical conductivity of the catalyst. The detailed procedure for the measurement of the electrical conductivity of catalyst can be found elsewhere^{2,3}. The catalyst was heated in an N_2 stream for 24 hrs and then in an O_2 stream for 24 hrs at 330°C , to stabilize the catalyst activity. A tubular flow reactor which was made of a pyrex glass tube was used under atmospheric pressure at the temperature range of $130\text{--}170^\circ\text{C}$. All gas components in the effluent streams were analyzed by three gas chromatographs to follow the transient state as continuously as possible. The intraparticle and external particle mass transfer effects were reconfirmed to be negligible by testing the catalytic activity as a function of catalyst particle size (20-42 and 80-100 mesh) or flow rate (160 and 320 ml/min), at the same W/F.

2-2. Computer Simulation

NEC PC-9800DS was used to simulate the transient response curves. A new software package based on C-language was developed for a personal computer simulation technique and was reconfirmed to be very useful.

3. EXPERIMENTAL RESULTS AND DISCUSSION

3-1. Kinetic Analysis of Steady State Rate Data

Curve I in Fig. 1 illustrates a typical example of steady state rate data on ZnO at 150°C . The rate clearly exhibits a maximum and a minimum which is an anomalous tendency as a function of P_{CO} , suggesting the simultaneous progression of multi-reaction pathways as has been reported in the photo-oxidation of secondary alcohol on ZnO ¹¹. Our speculation comes on that a Langmuir-Hinshelwood mechanism is available at P_{CO} lower than 0.2 atm (Region 1), whereas an Eley-Rideal mechanism becomes dominant at higher than 0.4 atm (Region 2).

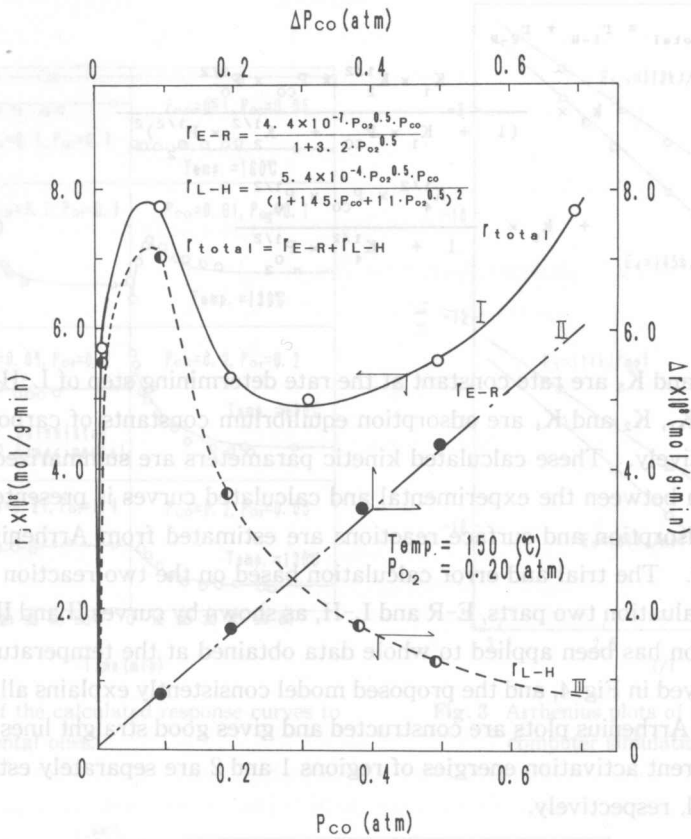
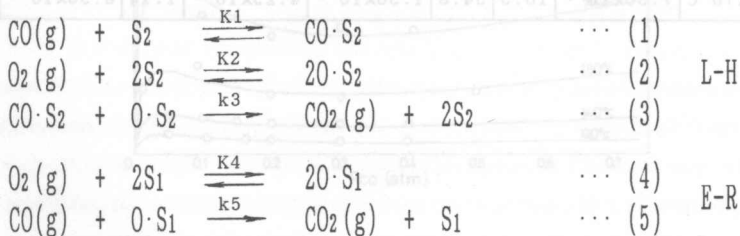


Fig. 1 Interpretation of the anomalous steady state rate data as a function of P_{CO} .
 Curve I : experimental steady state rate data.
 Curve II : experimental data evaluated by the transient response curve.
 Curve III : estimated by the difference $r_{total} - r_{E-R}$.

Temp. (°C)	k ₁	k ₂	k ₃	k ₄	k ₅
130	3.88 × 10 ⁻⁴	2.82	7.78 × 10 ⁻⁷	9.25 × 10 ⁻⁴	1.08
140	8.10 × 10 ⁻⁴	308	1.82 × 10 ⁻⁶	1.82 × 10 ⁻³	1.10
150	1.73 × 10 ⁻³	142	8.02 × 10 ⁻⁷	1.82 × 10 ⁻³	1.10
160	4.01 × 10 ⁻³	132	1.82 × 10 ⁻⁶	1.82 × 10 ⁻³	1.10
170	7.50 × 10 ⁻³	103	1.50 × 10 ⁻⁶	1.82 × 10 ⁻³	1.10

The reaction model can be proposed as follows.



Steps (1)-(3) are the L-H route and steps (4) and (5) are the E-R route. The rate determining step is step (3) for the L-H route and step (5) for the E-R route. Based on the multi-reaction pathway model, the total reaction rate (r_{total}) can be written as

$$\begin{aligned}
 r_{\text{total}} &= r_{\text{L-H}} + r_{\text{E-R}} \\
 &= k_3 \times \frac{K_1 \times K_2^{1/2} \times P_{\text{CO}} \times P_{\text{O}_2}^{1/2}}{(1 + K_1 \times P_{\text{CO}} + K_2^{1/2} \times P_{\text{O}_2}^{1/2})^2} \\
 &\quad + k_5 \times \frac{K_4^{1/2} \times P_{\text{CO}} \times P_{\text{O}_2}^{1/2}}{1 + K_4^{1/2} \times P_{\text{O}_2}^{1/2}} \tag{6}
 \end{aligned}$$

Where K_3 and K_5 are rate constant at the rate determining step of L-H and E-R routes, respectively. K_1 , K_2 and K_4 are adsorption equilibrium constants of carbon monoxide and oxygen respectively. These calculated kinetic parameters are summarized in Table 1 and the comparison between the experimental and calculated curves is presented in Fig. 2. All energies for adsorption and surface reactions are estimated from Arrhenius plots as illustrated in Fig. 3. The trial and error calculation based on the two reaction paths model are used for the evaluation two parts, E-R and L-H, as shown by curves II and III in Fig. 1. The same calculation has been applied to whole data obtained at the temperature range of 130-170°C as displayed in Fig. 4, and the proposed model consistently explains all of them. Using these data, the Arrhenius plots are constructed and gives good straight lines as shown in Fig. 5 and the apparent activation energies of regions 1 and 2 are separately estimated to be 105 and 121 kJ/mol, respectively.

Table 1. Summary of the calculated kinetic parameters.

temp.	k1, k2	K1	K2	k3	k4	K4	k5
130°C	3.88×10 ⁻⁵	249	382	7.76×10 ⁻⁸	9.25×10 ⁻⁶	105	1.85×10 ⁻⁸
140°C	8.10×10 ⁻⁵	198	208	1.62×10 ⁻⁷	2.63×10 ⁻⁵	30.4	5.26×10 ⁻⁸
150°C	1.73×10 ⁻⁴	145	113	3.46×10 ⁻⁷	6.85×10 ⁻⁵	10.1	1.37×10 ⁻⁷
160°C	4.01×10 ⁻⁵	122	65.1	8.02×10 ⁻⁷	1.63×10 ⁻⁴	3.1	3.25×10 ⁻⁷
170°C	7.50×10 ⁻⁵	10.3	34.8	1.50×10 ⁻⁶	4.25×10 ⁻⁴	1.14	8.50×10 ⁻⁷

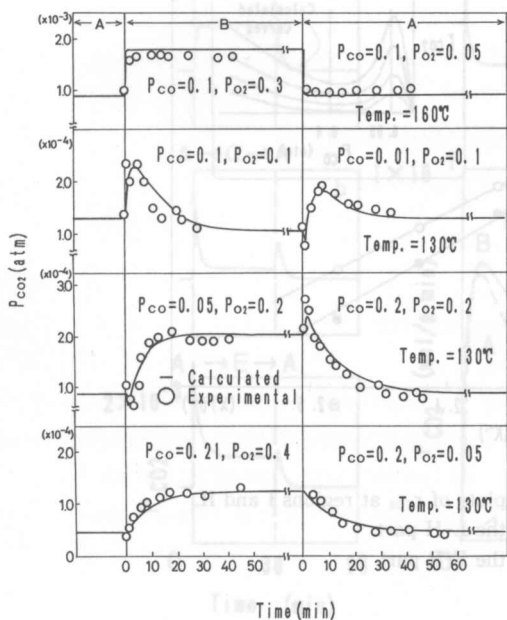


Fig. 2 Fitting of the calculated response curves to the experimental ones.

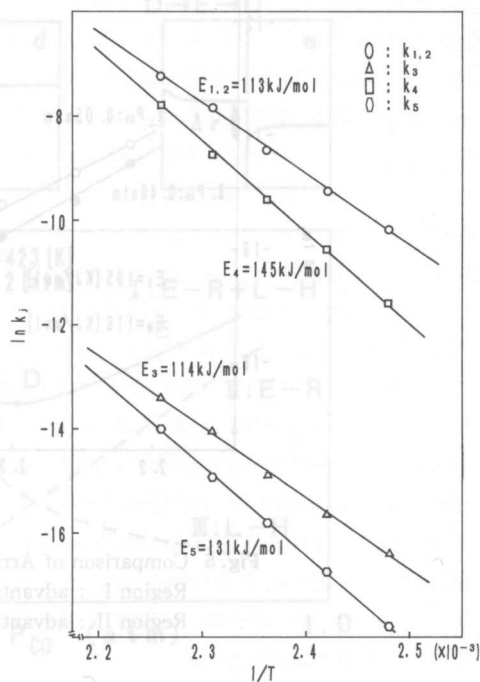


Fig. 3 Arrhenius plots of k_j evaluated by the computer simulation.

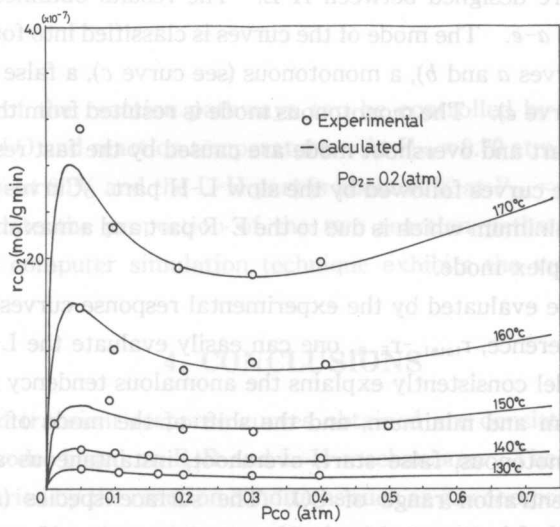


Fig. 4 Fitting of the proposed model to the steady state rate curves as a function of P_{CO} .

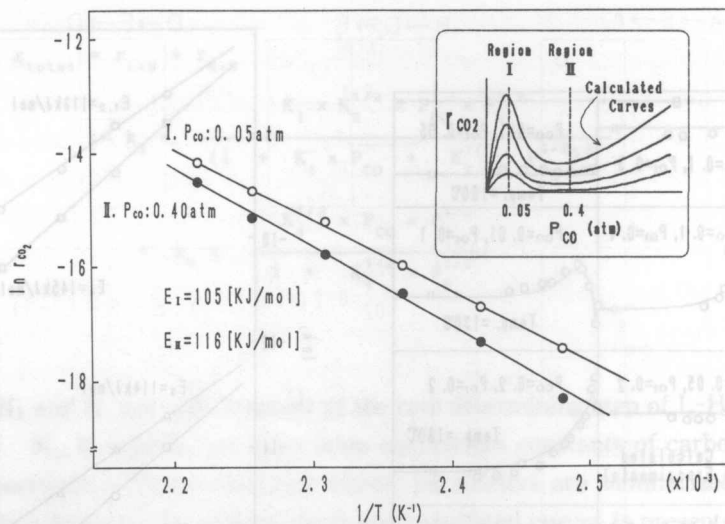


Fig. 5 Comparison of Arrhenius plots of r_{CO_2} at regions I and II.
 Region I : advantage of the L-H part.
 Region II : advantage of the E-R part.

3-2. Computer Simulation of Transient Response Curves

Five specified CO concentrations are marked on curve I as A-E in Fig. 1 and five transient experiments are designed between A-E. The results obtained are presented in Fig. 6 by response curves *a-e*. The mode of the curves is classified into four different types⁷, a complex mode (see curves *a* and *b*), a monotonous (see curve *c*), a false start (see curve *d*) and an overshoot (see curve *e*). The monotonous mode is resulted from the advantage of the L-H part. The false start and overshoot mode are caused by the fast response of E-R part at the initial stage of the curves followed by the slow L-H part. Curves *a* and *b* exhibit an anomalous behavior, a minimum which is due to the E-R part and a maximum due to the L-H part, indicating the complex mode.

The E-R part can be evaluated by the experimental response curves as shown in curve *e* by Δr . From the difference, $r_{total} - r_{E-R}$, one can easily evaluate the L-H part (see curve III). The proposed model consistently explains the anomalous tendency of the steady state rate data with maximum and minimum, and the shift of the mode of transient response curves between the monotonous, false start, overshoot, instantaneous and complex types depending on the concentration range of CO. The surface species (*Is*) controlling the reaction pathways may be considered to be surface oxygen species. In our previous paper³, it has been demonstrated that two adsorbed oxygen species O^- and O (neutral) are available for CO oxidation with the two reaction pathways on ZnO, each of which has different rate. Although we have no concrete experimental evidences discriminating the two species for the two paths, one may presume O^- to be available for the E-R part, because the change of electrical conductivity of catalyst during the reaction is fast corresponding to Δr in curve *e*.

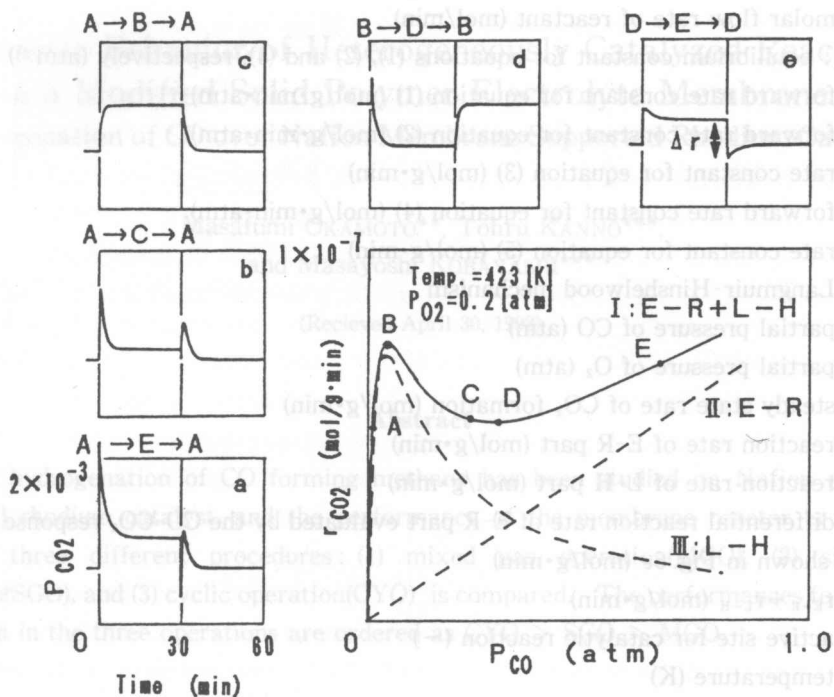


Fig. 6 Variation of the mode of transient response curve depending on the stepwise change regions between A, B, C, D and E in P_{CO} .

The selectivity of the reaction pathways can be controlled by CO concentration, the proportion of O^- and O and reaction temperature. At $P_{CO}=0.70$ atm and 150°C , the selectivity of E-R part is about 80% and the L-H part is about 90% at $P_{CO}=0.10$ atm. Accordingly one can easily regulate the proportion of the two reaction pathways due to the partial pressure of CO. A computer simulation technique exhibits the validity of the proposed model.

4. CONCLUSIONS

The complicated transient response curves obtained are consistently explained by the two path reaction model based on E-R and L-H mechanisms. The proportion of the two path is drastically varied by the reaction conditions such as gas composition and temperature. The lower P_{CO} and reaction temperature make the advantage of L-H route rather than the E-R route.

5. NOMENCLATURE

- E_j : activation energy for elementary step j (kJ/mol)
 E-R : Eley-Ridel mechanism

- F : molar flow rate of reactant (mol/min)
- K_1, K_2, K_4 : equilibrium constant for equations (1), (2) and (4), respectively (atm^{-1})
- k_1 : forward rate constant for equation (1) ($\text{mol/g}\cdot\text{min}\cdot\text{atm}$)
- k_2 : forward rate constant for equation (2) ($\text{mol/g}\cdot\text{min}\cdot\text{atm}$)
- k_3 : rate constant for equation (3) ($\text{mol/g}\cdot\text{min}$)
- k_4 : forward rate constant for equation (4) ($\text{mol/g}\cdot\text{min}\cdot\text{atm}$)
- k_5 : rate constant for equation (5) ($\text{mol/g}\cdot\text{min}$)
- L-H : Langmuir-Hinshelwood mechanism
- P_{CO} : partial pressure of CO (atm)
- P_{O_2} : partial pressure of O₂ (atm)
- r_{CO_2} : steady state rate of CO₂ formation ($\text{mol/g}\cdot\text{min}$)
- $r_{\text{E-R}}$: reaction rate of E-R part ($\text{mol/g}\cdot\text{min}$)
- $r_{\text{L-H}}$: reaction rate of L-H part ($\text{mol/g}\cdot\text{min}$)
- Δr : differential reaction rate of E-R part evaluated by the CO-CO₂ response curve as shown in Fig. 6e ($\text{mol/g}\cdot\text{min}$)
- r_{total} : $r_{\text{E-R}} + r_{\text{L-H}}$ ($\text{mol/g}\cdot\text{min}$)
- S : active site for catalytic reaction (-)
- T : temperature (K)
- W : weight of catalyst (g)

References

- 1) Kherbeche, A., Hubaut, R., Bonnelle, J. P. and Grimblet, J., *J. Catal.*, **131**, 204 (1991).
- 2) Kobayashi, M., Kobayashi, H. and Kanno, T., *Chem. Eng. Comm.*, **66**, 23 (1988).
- 3) Kobayashi, M., Kanno, T. and Kimura, T., *J. Chem. Soc. Faraday Trans. 1.*, **84**, 2099 (1988).
- 4) Kimura, T., Kanno, T., Hayashi, M. and Kobayashi, M., *Memoirs of the Kitami Institute of Technology*, **18**, 212 (1987).
- 5) Kobayashi, H. and Kobayashi, M., *Catal. Rev. Eng. Sci.*, **10**, 104 (1974).
- 6) Bennet, C. O., *Catal. Rev. Eng. Sci.*, **12**, 105 (1976).
- 7) Kobayashi, M., *Chem. Eng. Sci.*, **37**, 393 (1982).
- 8) Kobayashi, M., *J. Chem. Tech. Biotechnol.*, **29**, 552 (1979).
- 9) Kobayashi, M., Kobayashi, H., "Some Theoretical Problems of Catalysis", ed. by Kenji Tamaru, University Tokyo Press, 117 (1973).
- 10) Kobayashi, M., Kobayashi, H., *Bull. Chem. Soc. Japan*, **49**, 3008 (1976).
- 11) Cunningham, J., Hodnett, B. K., *J. Chem. Soc. Faraday Trans. 1*, **77**, 2277 (1981).
- 12) Matsuura, I., Kubokawa, Y. and Toyama, O., *Nippon Kagaku Zasshi*, **81**, 997 (1960).
- 13) Tanaka, K. and Blyholder, G., *JCS Chem. Comm.*, 736 (1971).
- 14) Ohtsuka, K., Tanaka, K. and Tamura, K., *Nippon Kagaku Zasshi*, **88**, 830 (1987).